ESI Preprints Not Peer-reviewed

Diachronic Analysis of the Irobo Classified Forest (Sikensi, Ivory Coast)

Kobenan Kadjo Raphael
Geomatics Specialist, Ph.D. in Geography, Identité et Différenciation des Espaces de l'Environnement et des Sociétés (IDEES), Université Le Havre Normandie, France
N'guessan Kouassi Fulgence
Associate Professor, Institut de Géographie Tropicale, Université Félix Houphouët-Boigny, Abidjan, Côte d'Ivoire
Banos Arnaud
CNRS – Université de Montréal CRM – CNRS ; IDEES (Identité et Différenciation des Espaces de l'Environnement et des Sociétés), Université Le Havre Normandie, Le Havre, France

Approved: 19 August 2026
Posted: 21 August 2026

Cite As:
Kobenan, K.R., N'guessan, K.F., & Banos, A. (2026). *Diachronic Analysis of the Irobo Classified Forest (Sikensi, Ivory Coast).* ESI Preprints.
https://doi.org/10.19044/esipreprint.8.2026.p495

Abstract

The decline in forest cover is a major conservation challenge in Côte d'Ivoire, where the expansion of agricultural activities exerts considerable pressure on forest ecosystems. This study analyzes the spatiotemporal dynamics of land use in the Irobo Classified Forest between 1988 and 2026 and proposes a trend-based scenario for forest cover change by 2050. The study used Landsat 4 TM and Landsat 8 OLI/TIRS satellite imagery processed in Google Earth Engine, supplemented by GIS data and field observations. Supervised classification using the Classification and Regression Trees (CART) algorithm was used to distinguish four land-use classes : water bodies, forest, cropland/fallow land, and settlements/bare land. The results reveal a substantial decline in forest cover, which decreased from 19105.81 ha (46.67%) in 1988 to 8278.17 ha (20.22%) in 2026, representing a loss of 10827.64 ha, or 56.67% of the initial forest cover. The average annual forest loss was estimated at 284.94 ha/year, corresponding to an annual deforestation rate of 2.20%. Meanwhile, cropland and fallow land increased from 50.69% to 79.10% of the total area of the classified forest. Spatial analysis also reveals fragmentation and reduced continuity of the remaining forest cover. According to the trend-based scenario, forest area could decline to approximately 4881.19 ha by 2050, representing 11.92% of the total area of the classified forest. These results highlight the importance of strengthening forest monitoring, conserving remaining forest areas, and implementing restoration measures to promote the sustainable management of the Irobo Classified Forest.

Keywords: Côte d'Ivoire, Irobo Classified Forest (Sikensi), deforestation, land use, remote sensing, GIS, spatial projection

1. Introduction

Tropical rainforests play a major role in ecosystem functioning, particularly through carbon storage, water cycle regulation, soil protection, and biodiversity conservation (Tao et al., 2022). However, these ecosystems have experienced significant decline over the past several decades due to the combined effects of human activities and environmental changes. Across tropical rainforest regions, forest loss has been estimated at approximately 220 million hectares since 1990 (Vancutsem et al., 2021; Bourgoin et al., 2024).

In Côte d'Ivoire, this trend is particularly pronounced. Dense rainforests, once widespread, have declined considerably, from approximately 16 million hectares in the 19th century to 2.97 million hectares in 2020 (Aké-Assi et al., 1990; Cuny et al., 2023).

This decline is mainly linked to agricultural expansion, bushfires, illegal logging, illegal gold mining, and other pressures on natural resources. Other contributing factors include population growth, urbanization, and challenges related to the sustainable management of forest areas (Kouassi, 2008; Koné et al., 2014; Andrieu et al., 2016; BNETD, 2016; N'Dri Ehikpa et al., 2020; Kobenan et al., 2021; Cuny et al., 2023).

The Irobo Classified Forest, located in southern Côte d'Ivoire, is an example of these changes. It faces increasing pressure from agricultural land clearing, forest resource exploitation, and the gradual settlement of populations engaged in cash crop farming, particularly cocoa and rubber. These activities contribute to changes in vegetation cover and highlight the challenges of conserving and sustainably managing classified forests in Côte d'Ivoire (Gueulou et al., 2020; N'Dri Ehikpa et al., 2020; Kouassi et al., 2023; Malan et al., 2023).

Despite these pressures, understanding their extent requires information on forest cover changes over a sufficiently long period. In this context, diachronic analysis of land use helps identify changes in the landscape and assess the extent of areas converted for human activities. The combined use of remote sensing, geographic information systems (GIS), and field observations provides a suitable approach for monitoring changes in forest cover and identifying the main forms of land conversion.

This study aims to analyze spatiotemporal changes in land use in the Irobo Classified Forest between 1988 and 2026. More specifically, it seeks to: (i) map the main land-use classes for the study years; (ii) quantify changes in forest cover; (iii) identify the main forms of human pressure observed in the classified forest; and (iv) analyze, based on trends observed between 1988 and 2026, the likely evolution of forest cover by 2050.

2. Study Area

The Irobo Classified Forest is located in southern Côte d’Ivoire, between the Sikensi Department and the Bandama River (Figure 1). Covering an area of 40940 hectares, it extends across the departments of Dabou, Grand-Lahou, Sikensi, and Tiassalé. Its geographical extent ranges from 962021.52 to 983830.31 m for the X coordinate (Easting) and from 600680.47 to 637907.91 m for the Y coordinate (Northing), in the WGS 84 / UTM Zone 29N coordinate system (EPSG:32629). It is accessible by a main road connecting Bécédi to Ahouanou, passing through Bakanou A and Bakanou B, as well as the forest camps of Brikisso and Pikinou. A road to the north provides access to Akalékro, on the banks of the Bandama River, while an old road west of Bécédi provides access to the northeastern part of the forest area.

The Irobo Classified Forest lies within the humid tropical zone. It is mainly characterized by two types of soil: sandy-clay soils rich in quartz and developed on schist, and soils derived from granitic formations with a coarser texture (De Boissezon, 1967; Perraud, 1971). The terrain is gently rolling and consists of small hills with slopes generally ranging from 5 to 10%. These hills are 20 to 30 m high, with elongated forms and semi-interfluves ranging from 500 to 800 m in width (De Boissezon, 1967).

The area has a humid equatorial climate. Annual rainfall ranges from 1600 to 1800 mm, while the average temperature is approximately 26.5 °C. These climatic conditions favor the development of dense, humid vegetation adapted to the ecological conditions of southern Côte d’Ivoire.

The area is mainly inhabited by populations engaged in agriculture. These include the indigenous Abidji people as well as migrant communities, including the Baoulé, Agni, and Lobi. Agriculture is one of the main activities in the area, particularly through the development of cocoa, rubber, oil palm, and coffee plantations.

Since it was classified in 1962, the Irobo Classified Forest has been subject to increasing pressure, particularly from the expansion of agricultural activities and the gradual occupation of certain parts of the forest. Land clearing for plantations and conflicts over land occupation contribute to the gradual transformation of the forest landscape. These pressures represent an important challenge for forest conservation and justify the analysis of long-term changes in land use.

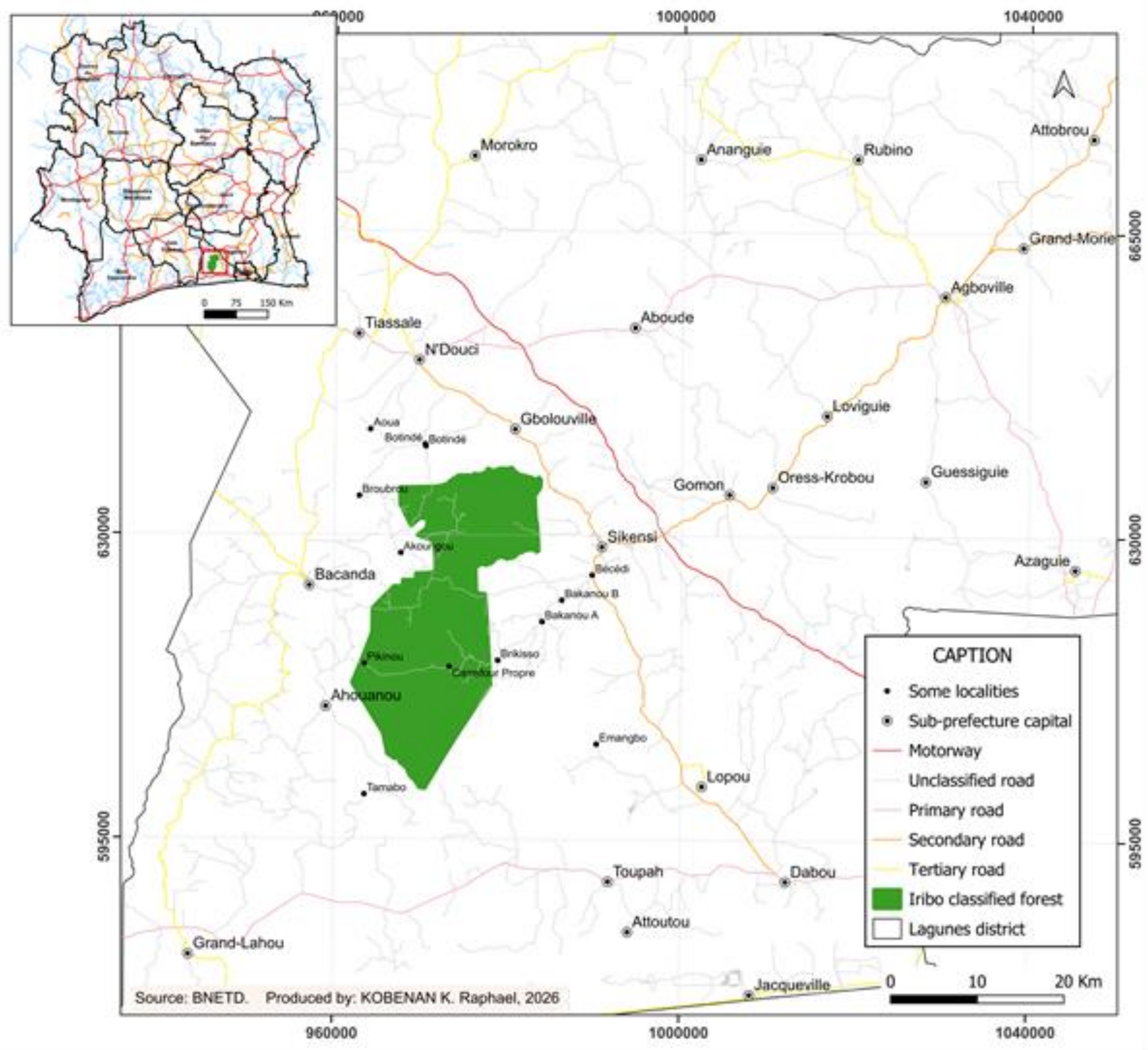

Figure 1 : Location of the Irobo Classified Forest

3. Materials and Methods

3.1. Data

The analysis of land-use dynamics in the Irobo Classified Forest is based mainly on Landsat satellite imagery, vector data delineating the classified forest, and reference data used for training and validating the classifications. Two dates were selected to assess changes in land use over a 38-year period: 1988 and 2026.

For 1988, a Landsat 4 image acquired by the Thematic Mapper (TM) sensor on December 24, 1988, was used. It corresponds to WRS-2 Path/Row 196/056 and has the product identifier LT04_L2SP_196056_19881224_20200917_02_T1. For 2026, the analysis is based on a Landsat 8 OLI/TIRS Collection 2 Level-2 image acquired on March 12, 2026. It also corresponds to WRS-2 Path/Row 196/056 and has the product identifier LC08_L2SP_196056_20260312_20260314_02_T1. This image has a cloud cover of 1.19%, allowing a clear observation of the study area.

Both images were acquired during the main dry season, which extends from December to April in the study area.

Within this period, priority was given to scenes with low cloud cover over the classified forest in order to reduce atmospheric effects and seasonal differences that could affect the land-use analysis. This approach led to the selection of the December 1988 image and the March 2026 image.

For the classification, six spectral bands were selected for each date. For Landsat 4 TM, these were bands SR_B1, SR_B2, SR_B3, SR_B4, SR_B5, and SR_B7, corresponding respectively to blue, green, red, near-infrared (NIR), short-wave infrared 1 (SWIR1), and short-wave infrared 2 (SWIR2). For Landsat 8 OLI, bands SR_B2, SR_B3, SR_B4, SR_B5, SR_B6, and SR_B7 were used; they correspond to the same spectral ranges. This selection provides comparable spectral variables between the two sensors for land-use classification.

The map data were obtained from the Center for Geographic and Digital Information of the National Office for Technical Studies and Development (BNETD). They include administrative boundaries, the road network, localities, and other elements needed to delineate and map the study area. The boundary of the Irobo Classified Forest was provided in vector format and used to delineate the analysis area. It covers an area of 40940 ha.

The field data consist of georeferenced points recorded using a GPS and photographs. They were used to identify the main land-use classes observed in the classified forest and to support the interpretation of satellite imagery, as well as the training and validation of the classifications.

3.2. Preprocessing of Satellite Images

The satellite images were preprocessed in the Google Earth Engine (GEE) environment using Landsat Collection 2, Level-2 surface reflectance products. The scale factors associated with these products were applied to the optical bands to obtain the reflectance values used for subsequent processing. Pixels that could affect data quality were masked using the QA_PIXEL and QA_RADSAT quality bands. The mask excluded fill pixels, clouds, dilated clouds, cloud shadows, and pixels affected by radiometric saturation. For the Landsat 8 image, pixels identified as cirrus clouds were also excluded. This step was used to reduce the influence of atmospheric and radiometric effects on the spectral values used for classification. Processing was performed at a spatial resolution of 30 m for both dates to ensure spatial comparability. A false-color composite combining SWIR1, near-infrared (NIR), and blue bands was also used to facilitate visual interpretation of the images, particularly to distinguish vegetation from agricultural areas during the creation of training samples (O'Neill et al., 1996).

3.3. Sampling and Land-Use Nomenclature

The land-use classification is based on a supervised approach (Bonn et al., 1992 ; Kobenan et al., 2021). Four classes were defined based on the main land-use types observed in the classified forest (Table 1).

Table 1 : Nomenclature of land-use classes used for classification

Code	Class
1	Water bodies
2	Forest
3	Cropland/Fallow land
4	Settlements/Bare land

The reference samples were obtained from GPS points recorded in the field, visual interpretation of satellite imagery, and available information on the study area. For each date, 250 reference points were used to delineate the training polygons and were distributed across the four land-use classes : 50 for water bodies, 90 for forest, 65 for cropland/fallow land, and 45 for settlements/bare land. However, the « Water bodies » class requires special attention. Water bodies in the classified forest consist mainly of temporary watercourses, some of which may dry up during the dry season. Their limited presence in satellite images acquired during this period does not necessarily mean that they are absent on the ground.

The reference polygons were then sampled at a spatial resolution of 30 m to extract the spectral values of pixels corresponding to the different land-use classes.

To reduce imbalance among the classes and prevent a highly represented class from dominating the classifier training, the number of samples was limited to 3000 pixels per class. The balanced samples were then randomly divided into two subsets: 70% for training and 30% for validation.

3.4. Supervised Classification and Validation

Land-use mapping was performed using the Classification and Regression Trees (CART) algorithm available in Google Earth Engine. For each of the two dates, the balanced samples were randomly divided into two distinct subsets: 70% were used to train the classifier, while the remaining 30% were reserved for validation. The samples used for validation were therefore not used to train the model. After training, the CART model was applied to the selected spectral bands of each image to produce a map showing the four land-use classes defined previously. A 3 × 3-pixel majority filter (focal_mode) was then applied to the classified images to reduce the "salt-and-pepper" effect and improve the spatial continuity of the mapped units.

The quality of the classifications was evaluated using the samples reserved for validation and a confusion matrix. Classification performance was assessed mainly using overall accuracy and the Kappa coefficient (Konan et al., 2016), calculated using the equations presented below. The 1988 classification had an overall accuracy of 97.79% and a Kappa coefficient of 0.971, while the 2026 classification had an overall accuracy of 98.01% and a Kappa coefficient of 0.966. These results indicate a high level of agreement between the classes assigned by the model and the reference data used for validation.

$$\hat{k} = \frac{a - b}{1 - b} \qquad a = \frac{1}{N}\sum_{i=1}^{Nc} x_{ii} \qquad b = \frac{1}{N}\sum_{i=1}^{Nc}(x_{+i} \cdot x_{i+})$$

Where :

Nc = Number of classes

N = Total number of observations

xii = Number of observations in column i, row i (diagonal of the matrix)

x+i = Total number of observations in column i

xi+ = Total number of observations in row i

3.5. Calculation of Areas and Change Analysis

The area occupied by each land-use class was calculated from the classified pixels. The area of each pixel was converted to hectares and then aggregated within the boundaries of the classified forest.

Given the slight difference between the geometric area of the vector file (41118.29 ha) and the official area of the classified forest (40940 ha), the calculated areas were normalized to the official area. This process preserves the relative proportions obtained from the classifications while ensuring that the sum of the areas of the different classes corresponds exactly to 40940 ha for each study year.

Forest dynamics between 1988 and 2026 were assessed based on changes in forest area. Total forest loss (P), expressed in hectares, was calculated using the following equation :

$$P = S_{1988} - S_{2026}$$

where S_{1988} and S_{2026} represent the forest areas in 1988 and 2026, respectively.

The average annual forest loss (Pm), expressed in hectares per year, was calculated as follows :

$$P_m = \frac{(S_{1988} - S_{2026})}{(2026 - 1988)}$$

The annual deforestation rate (θ), expressed as a percentage per year, has sometimes been estimated by dividing the deforestation rate observed over a given period by the duration of that period (Menon & Bawa, 1997 ; Narendra Prasad, 1998). However, this approach does not adequately represent the annual rate of change in forest cover (Puyravaud, 2003 ; Vieilledent et al., 2013). In this study, the annual rate of change in forest cover was calculated over the 38 years between the two observations using the approach proposed by Puyravaud (2003). To express deforestation as a positive value when forest area decreases, the sign of the rate of change was reversed. The annual deforestation rate was therefore calculated using the following equation :

$$\theta = -\frac{1}{38}\ln\left(\frac{S_{2026}}{S_{1988}}\right) * 100$$

where ln denotes the natural logarithm. Thus, a positive value of θ indicates a decrease in forest area over the study period. This approach provides an estimate of the average annual rate of forest cover loss over the entire study period.

3.6. Projection of Forest Cover by 2050

The potential change in forest cover by 2050 was estimated based on the dynamics observed between 1988 and 2026. The projection was based on an exponential extrapolation of forest cover change and was considered a trend-based scenario. First, the ratio between the forest areas observed in 2026 and 1988 was calculated using the following equation :

$$R = \frac{S_{2026}}{S_{1988}}$$

The forest cover retention coefficient between 2026 and 2050 was then determined by considering the duration of the historical period (1988–2026) and the projection period (2026-2050) :

$$R_{2050} = R^{\frac{2050-2026}{2026-1988}}$$

The theoretical forest area by 2050 was then estimated as follows :

$$S_{2050} = S_{2026} \times R_{2050}$$

This approach assumes that the relative rate of forest cover change observed between 1988 and 2026 will continue through 2050.

The resulting value is therefore not a certain prediction of the future state of the forest, but a trend-based scenario used to assess its potential change if the observed dynamics continue.

A spatial allocation of the projected forest loss was then carried out in Google Earth Engine to produce a map of land use by 2050. This allocation was applied to pixels classified as forest in 2026 using a vulnerability index combining proximity to non-forest areas and local human pressure.

First, a mask distinguishing forest pixels from non-forest pixels was created from the 2026 classification. The distance from each forest pixel to non-forest areas was then calculated at a spatial resolution of 30 m. This distance was converted into a proximity index using the following equation :

$$P_r = \frac{1}{d+1}$$

where d represents the distance to the nearest non-forest pixel. This transformation assigns the highest values to forest pixels located close to areas that are already non-forest. The proximity index was then normalized between 0 and 1 based on the minimum and maximum values observed within forest areas :

$$P = \frac{P_r - P_{min}}{P_{max} - P_{min}}$$

Local human pressure (A) was estimated as the average proportion of non-forest pixels within a 300 m circular neighborhood around each pixel. This variable ranges from 0, corresponding to an entirely forested neighborhood, to 1, corresponding to an entirely non-forest neighborhood. The vulnerability index (V) was then calculated by assigning equal weights to the two components :

$$V = 0{,}5P + 0{,}5A$$

where P represents the normalized proximity to non-forest areas and A represents local human pressure. High values of V therefore correspond to forest pixels considered most exposed to potential conversion.

To spatially allocate the forest area expected to be lost between 2026 and 2050, a vulnerability threshold was identified using a binary search procedure with 30 iterations. For each threshold tested, the area of forest pixels with a vulnerability value greater than or equal to the threshold was calculated and compared with the theoretical forest loss obtained from the exponential projection. The final threshold was selected to minimize the difference between the area to be converted on the map and the projected theoretical loss. A very small random value was added to the index only when ranking the pixels to separate pixels with identical vulnerability values. Forest pixels selected as potentially deforested were then reclassified as “Cropland/Fallow land” to produce the projected land-use map for 2050.

Finally, the forest area obtained from the projected 2050 map was compared with the theoretical forest area obtained from the exponential extrapolation. The difference between these two values was calculated to assess the agreement between the quantitative projection and its spatial allocation. The results of this comparison are presented in the Results section.

After preprocessing, classification, and analysis, the resulting spatial data were imported into the GIS environment (ArcGIS) for formatting and map production. This step was used to produce the land-use maps for 1988 and 2026, as well as the projected map for 2050. The map layout involved organizing the different information layers and adding the elements needed to read and interpret the maps.

4. Results

4.1. Classification Performance

The supervised classifications performed for 1988 and 2026 showed high levels of accuracy. For 1988, the overall accuracy was 97.79%, with a Kappa coefficient of 0.971. For 2026, the overall accuracy was 98.01%, with a Kappa coefficient of 0.966. These results indicate a high level of agreement between the classes obtained from the classification and the reference data used for validation.

4.2. Status and Changes in Land Use Between 1988 and 2026

The results show significant changes in land use within the Irobo Classified Forest between 1988 and 2026 (Table 2 ; Figure 2). In 1988, forest covered 19105.81 ha, representing 46.67% of the study area. Cropland and fallow land represented the largest land-use class, covering 20753.18 ha, or 50.69% of the total area. The « Settlements/Bare land » class covered 1081.01 ha, representing 2.64% of the classified forest area. In 2026, forest area decreased to 8278.17 ha, or 20.22% of the total area. In contrast, cropland and fallow land covered 32384.58 ha, representing 79.10% of the study area. The « Settlements/Bare land » class covered only 277.25 ha, or 0.68% of the total area.

Table 2 : Changes in land use in the Irobo Classified Forest between 1988 and 2026

Land Use Classes	1988 (ha)	1988 (%)	2026 (ha)	2026 (%)	Change (ha)
Water bodies	0.00	0.00	0,00	0,00	0.00
Forest	19 105.81	46.67	8 278.17	20.22	**-10 827.64**
Cropland/Fallow land	20 753.18	50.69	32 384.58	79.10	**11 631.40**
Settlements/Bare land	1 081.01	2.64	277.25	0.68	**-803.76**
Total	**40 940**	**100**	**40 940**	**100**	-

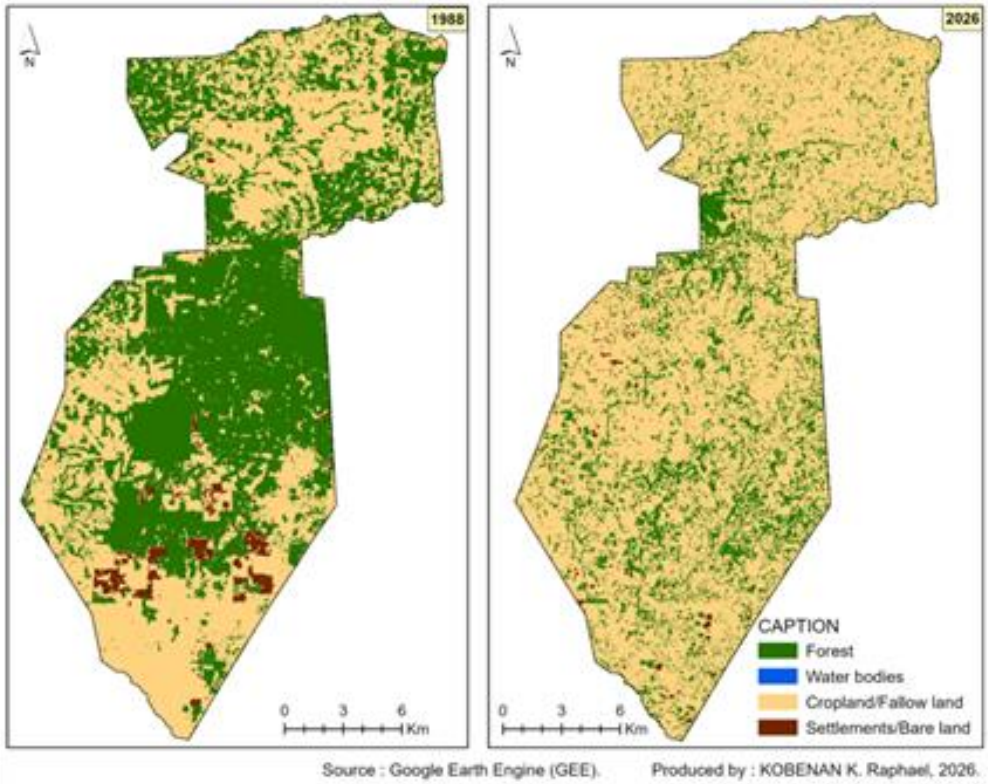

Figure 2 : Land Use in 1988 and 2026

The observed changes were mainly characterized by a significant decline in forest cover and a sharp increase in cropland and fallow land. Between 1988 and 2026, forest area decreased by 10827.64 ha, representing a 56.67% reduction compared with its 1988 area. At the same time, cropland and fallow land increased by 11631.40 ha. This expansion of agricultural areas was also observed in the field. Field observations showed the presence of agricultural plantations within the classified forest, particularly cocoa trees associated in some areas with banana trees (Photo 1). Camps and dwellings were also observed near or within these cultivated areas (Photo 2). These observations show the importance of agricultural activities and the presence of human settlements within the Irobo Classified Forest.

Photo 1: Cocoa and banana plantations observed near camps in the Irobo Classified Forest (January 2026)

Source : Photographs by KOBENAN K. Raphaël, January 2026.

Photo 2: Examples of camps observed in the Irobo Classified Forest (January 2026)

Source : Photographs by KOBENAN K. Raphaël, January 2026.

Over the 38 years between the two observations, the average annual forest loss was estimated at 284.94 ha/year, while the annual deforestation rate was 2.20% per year. These results show the significant decline in forest cover during the study period.

For water bodies, no measurable area was obtained for either study year. This can be explained by the mainly temporary nature of the watercourses in the study area, some of which dry up during the dry season. Since the satellite images were acquired in December 1988 and March 2026, these water bodies were not sufficiently represented to form measurable mapping units at a spatial resolution of 30 m.

The « Settlements/Bare land » class also decreased, from 1081.01 ha (2.64%) in 1988 to 277.25 ha (0.68%) in 2026, representing a reduction of 803.76 ha. This change may be linked to clearance operations that led to the removal of several camps within the classified forest. However, field observations indicate that some camps remain within the plantations. Due to their small size and their location within areas covered by vegetation, these settlements may be difficult to detect in Landsat images at a spatial resolution of 30 m. The mapped decrease in the « Settlements/Bare land » class therefore does not necessarily mean that all human settlements within the classified forest have disappeared.

4.3. Spatial Dynamics of Deforestation Between 1988 and 2026

The analysis of the spatial distribution of deforestation between 1988 and 2026 shows a decline in forest cover in different parts of the Irobo Classified Forest (Figure 3). Deforested areas are found both along the edges and within the classified forest, showing that forest loss was not limited to peripheral areas. In the central part of the classified forest, deforested areas are particularly extensive and cover large areas in some places. The remaining forest areas appear as small, scattered patches. This distribution shows a gradual fragmentation of forest cover and a reduction in its continuity.

In the northern part, deforested areas are also numerous but more widely dispersed. Some forest areas remain in this part of the classified forest, but they are often separated from one another. Overall, the map shows that deforestation between 1988 and 2026 led to a reduction and fragmentation of forest cover in the Irobo Classified Forest. The remaining forest areas are now more scattered and largely surrounded by non-forest areas.

Figure 3 : Spatial Dynamics of Deforestation in the Irobo Classified Forest Between 1988 and 2026

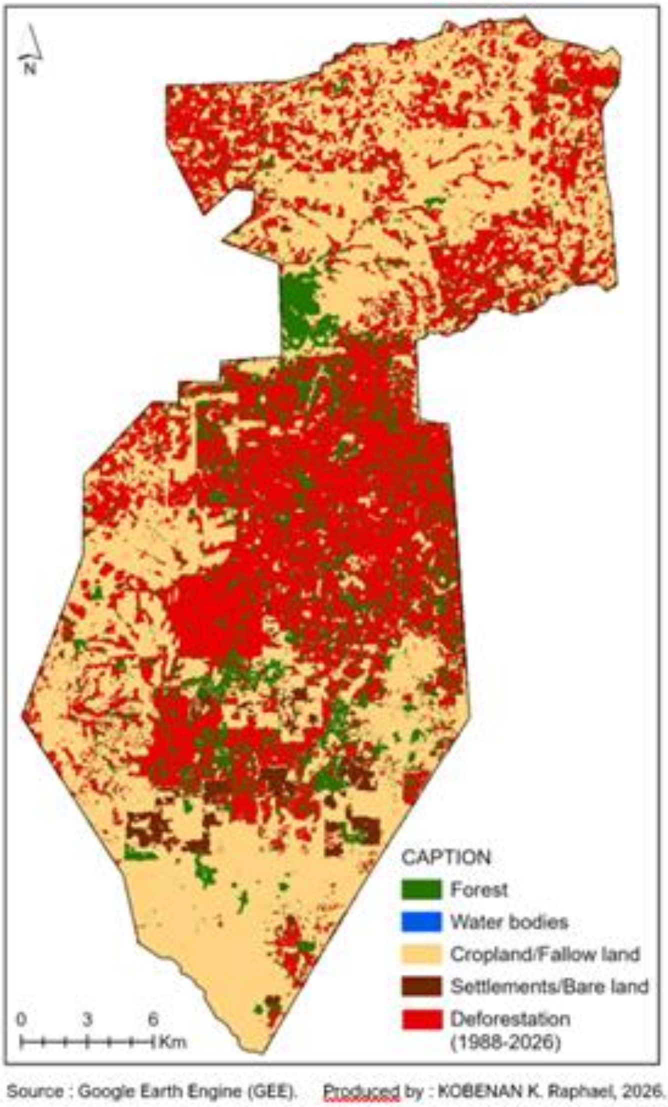

4.4. Projected Changes in Forest Cover by 2050

The trend-based projection indicates a continued decline in forest cover by 2050 (Figure 4). The theoretical forest area would decrease from 8278.17 ha in 2026 to 4881.19 ha in 2050, representing 11.92% of the total area of the Irobo Classified Forest. This change would correspond to an additional loss of approximately 3396.98 ha between 2026 and 2050, representing a 41.04% reduction in the forest cover present in 2026.

Figure 4 : Vulnerability to deforestation, projected deforestation between 2026 and 2050, and projected forest cover by 2050 in the Irobo Classified Forest

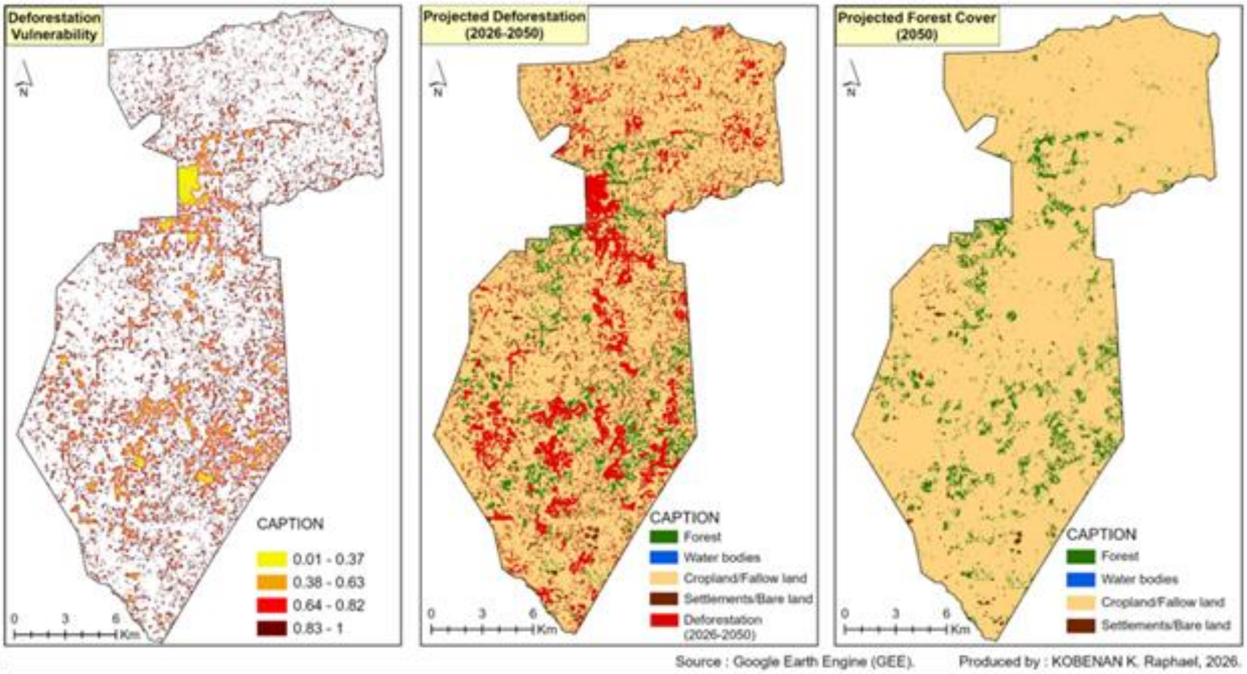

The spatial allocation of this loss results in a mapped forest area of 4858.16 ha in 2050. The difference from the projected theoretical forest area is 23.02 ha, or approximately 0.47%. This small difference indicates good agreement between the area obtained from the quantitative projection and that obtained after spatial allocation.

The vulnerability map shows an uneven distribution of areas that could be affected by deforestation. The highest vulnerability levels are scattered across different parts of the remaining forest areas. They are particularly present in the central and southern parts of the classified forest, but also appear in several areas in the northern part. The presence of high or moderate vulnerability levels within some forest areas shows that the potentially affected areas are not limited to the edges of the classified forest.

Projected deforestation between 2026 and 2050 also shows a wide spatial distribution. Areas that could lose their forest cover are found near cropland and fallow land, but also within some forest areas still present in 2026. The central part, which connects the two main sections of the classified forest, has a high concentration of areas projected to be deforested. In the southern part, potential losses appear more scattered and are associated with the remaining forest areas.

By 2050, cropland and fallow land would occupy most of the classified forest, while the remaining forest cover would consist of areas of different sizes scattered throughout the classified forest. Some forest areas would remain mainly in the central and southern parts, while the projected forest areas in the northern part would be smaller and more isolated.

Thus, assuming that the trend observed between 1988 and 2026 continues, deforestation could lead not only to a further reduction in forest area but also to greater fragmentation and a decrease in the spatial continuity of the remaining forest cover. Under this scenario, areas with the highest levels of vulnerability could require particular attention for monitoring and conservation.

However, these results should be interpreted as a trend-based scenario and not as a certain prediction of the state of the classified forest in 2050. The actual change in forest cover may depend on conservation and restoration measures, agricultural practices, management of the classified forest, and, more broadly, changes in human pressures.

5. Discussion

The diachronic analysis of land use shows a sharp decline in forest cover in the Irobo Classified Forest between 1988 and 2026. Forest area decreased from 19105.81 ha in 1988 to 8278.17 ha in 2026, representing a loss of 10827.64 ha, or 56.67% of the initial forest cover. This change represents an average loss of 284.94 ha/year and an annual deforestation rate of 2.20%. At the same time, cropland and fallow land increased from 20753.18 ha (50.69%) to 32384.58 ha (79.10%) of the classified forest area. These results show a significant decline in forest cover accompanied by a marked increase in agricultural land.

This change is consistent with field observations, which showed the presence of plantations, particularly cocoa and banana plantations, as well as camps within the classified forest. It suggests that agricultural activities are an important source of pressure on forest areas. This situation is similar to the findings of Malan et al. (2023) in the Goin-Débé Classified Forest, where a significant reduction in forest areas was observed between 1988 and 2020, along with the expansion of agricultural plantations and fallow land. Despite differences in the study sites and observation periods, these results show the importance of changes related to agricultural land use in several classified forests in Côte d'Ivoire.

Similar changes have also been reported in other tropical regions. Nourtier and Grinand (2016a) reported changes in forest cover in Mikea National Park in Madagascar, while Kimvula et al. (2023) showed the importance of agricultural activities in land-use dynamics at the INÉRA Kiyaka forest station in the Democratic Republic of the Congo. In Côte d'Ivoire, studies by Cuny et al. (2023), N'Dri Ehikpa et al. (2020), Kobenan et al. (2021), and Konan et al. (2016) also report changes in forest areas due to human activities, particularly the expansion of agricultural land. The changes observed in the Irobo Classified Forest are therefore part of a broader pattern of pressure on tropical forests.

Beyond the reduction in forest area, the spatial analysis conducted in Irobo shows that forest loss occurred in different parts of the classified forest and was not limited to its edges. The forest areas still present in 2026 appear more scattered and less continuous than in 1988. This pattern indicates fragmentation of forest cover, which could increase the vulnerability of the remaining forest areas. However, since the study did not use specific landscape fragmentation indices, this change should mainly be interpreted in terms of a decrease in forest area and the spatial continuity of forest cover.

The decrease in the « Settlements/Bare land » class observed between 1988 and 2026 should be interpreted with caution. Field observations show that camps remain within the classified forest, particularly within or near plantations. Their small size and location within areas covered by vegetation may make them difficult to detect in Landsat images at a spatial resolution of 30 m.

The decrease in this class on the maps therefore does not necessarily reflect a similar decrease in human presence within the classified forest. This limitation shows the importance of combining satellite analysis with field observations when interpreting land-use changes.

The results of the projection to 2050 follow the same trend. Assuming that the relative rate observed between 1988 and 2026 continues, the theoretical forest area could reach approximately 4881.19 ha in 2050, representing 11.92% of the classified forest area. This would represent an additional loss of approximately 3396.98 ha compared with 2026. The spatial allocation of this loss also shows that several forest areas still present in 2026 are vulnerable to conversion, particularly in the central and southern parts of the classified forest. If this trend continues, fragmentation could increase and the continuity of the remaining forest areas could be further reduced.

However, this projection should be considered a trend-based scenario rather than a certain prediction. It is based on the assumption that the relative trend observed between 1988 and 2026 will continue through 2050. It therefore does not directly take into account possible future changes in conservation policies, agricultural practices, forest restoration activities, or, more broadly, human pressures. Its main purpose is to identify a possible future trend and the areas that could be particularly exposed if current trends continue.

In this context, the results show the importance of strengthening conservation measures and the sustainable management of the Irobo Classified Forest. The observed decline in forest cover, the expansion of agricultural areas, and the vulnerability of some remaining forest areas show the importance of regular land-use monitoring, protecting the remaining forest areas, and strengthening restoration activities. It is also important to consider agricultural activities and the populations living in and around the forest when developing management strategies that combine forest conservation with local uses.

Conclusion

This study analyzed spatiotemporal changes in land use in the Irobo Classified Forest between 1988 and 2026 using Landsat satellite imagery, remote sensing and GIS tools, supplemented by field observations. The results show a sharp decline in forest cover over the 38-year study period. Forest area decreased from 19105.81 ha in 1988, representing 46.67% of the total area of the classified forest, to 8278.17 ha in 2026, representing 20.22%. This change corresponds to a loss of 10827.64 ha, or 56.67% of the 1988 forest cover, with an average annual loss of 284.94 ha/year and an estimated annual deforestation rate of 2.20%.

Along with the decline in forest cover, cropland and fallow land increased significantly, from 50.69% of the study area in 1988 to 79.10% in 2026. Field observations, particularly the presence of agricultural plantations and camps within the classified forest, support the results of the satellite analysis and show the importance of human activities in the current land use of this area. The spatial analysis also shows that forest loss was not limited to the edges of the classified forest but occurred in different parts of the area. The forest areas still present in 2026 appear more scattered and less continuous, indicating a gradual fragmentation of forest cover.

The trend-based projection for 2050 indicates that, if the trend observed between 1988 and 2026 continues, forest area could reach approximately 4881.19 ha, or 11.92% of the total area of the classified forest. This would correspond to an additional loss of approximately 3396.98 ha compared with 2026. However, this projection should be considered a trend-based scenario rather than a certain prediction, as future changes in forest cover may be influenced by conservation policies, agricultural practices, restoration activities, and changes in human pressures.

These results confirm the value of remote sensing and GIS for long-term land-use monitoring and for identifying forest areas that may be more exposed to change. Given the extent of the observed forest loss and the trend shown by the 2050 scenario, strengthening forest cover monitoring, protecting the remaining forest areas, and implementing restoration activities are important for the sustainable management of the Irobo Classified Forest.

Conflict of Interest: The authors reported no conflict of interest.

Data Availability: All data are included in the content of the paper.

Funding Statement: The authors did not obtain any funding for this research.

References:

1. Aké-Assi, L., & Boni, D. (1990). Développement agricole et protection de la forêt : quel avenir pour la forêt ivoirienne ? [Agricultural development and forest protection: What future for Côte d'Ivoire's forests?]. In: Ihlenfeldt, H.-D, H. Baijnath, M. Cheek, F. N. Hepper, J. Lejoly, G. L. Lucas, F. P. Malaisse, C. R. Peters, & D. C. J. Wessels (eds.), Proceedings of the twelfth plenary meeting of aetfat. Hamburg, September 4-10, 1988 (pp.169-176.). Mitt. Inst. Allg. Bot. Hamburg 23a.
2. Andrieu, J., Barima, Y.S., Diego, M., Vignal, M., & Zerbo, R., (2016). De l'enquête à la modélisation rétro-prospective (2001-2015) de la déforestation de la Forêt Classée du Haut Sassandra dans un contexte de conflit armé (Côte d'Ivoire) [From survey to retrospective and prospective modeling (2001–2015) of deforestation in the Haut-Sassandra Classified Forest in a context of armed conflict (Côte d'Ivoire)]. Colloque Changements socio-environnementaux et dynamiques rurales en Afrique de l'Ouest, Paris, France. ⟨hal-01343548⟩.
3. BNETD (Bureau national d'études techniques et de développement). (2016). Analyse qualitative des facteurs de déforestation et de dégradation des forêts en Côte d'Ivoire [Qualitative analysis of the drivers of deforestation and forest degradation in Côte d'Ivoire]. Rapport final. Abidjan, Côte d'Ivoire, 114 p. https://www.nitidae.org/files/b24e760c/161216081210_161214_analyse_facteurs_def_deg_ci_rapport_final.pdf.
4. Bonn, F., & Rochon, G. (1992). Précis de télédétection. Principes et méthodes [Remote sensing : Principles and methods] Presse universitaire du Québec, AUPELF, 484 p.
5. Bourgoin, C., Ceccherini, G., Girardello, M., Vancutsem, C., Avitabile, V., Beck, P. S. A., Beuchle, R., Blanc, L., Duveiller, G., Migliavacca, M., Vieilledent, G., Cescatti, A. & Achard, F. (2024). Human degradation of tropical moist forests is greater than previously estimated. Nature, 631, 570–576. https://doi.org/10.1038/s41586-024-07629-0.
6. Cuny, P., Plancheron, F., Bio, A., Kouakou, E. & Morneau, F. (2023). La forêt et la faune de Côte d'Ivoire dans une situation

alarmante – Synthèse des résultats de l'Inventaire forestier et faunique national [Forests and wildlife in Côte d'Ivoire in an alarming situation : Summary of the results of the National Forest and Wildlife Inventory]. Bois et Forêts des Tropiques, 355, 47-72. https://doi.org/10.19182/bft2023.355.a36939.

7. De Boissezon, P. (1967). Étude de reboisement et de protection des sols : Étude pédologique de la zone vulnérable de l'Irobo [Reforestation and soil protection study: Soil study of the vulnerable Irobo area]. Office de la Recherche Scientifique et Technique Outre-Mer, Centre d'Adiopodoumé, Ministère de l'Agriculture (Côte d'Ivoire), 214 p.
8. Gueulou, N., Coulibaly, B., Ouattara, N.D., N'Guéssan, A.K., Ahoba, A., & Bakayoko, A. (2020). Modes de gestion et efficacité de conservation des reliques de forêts naturelles en zone tropicale sèche : cas du Département de Korhogo (Nord, Côte d'Ivoire) [Management methods and conservation effectiveness of natural forest remnants in the dry tropical zone: The case of Korhogo Department (northern Côte d'Ivoire)]. International Journal of Biological and Chemical Sciences, 13(7), 3332-3346. https://doi.org/10.4314/ijbcs.v13i7.28.
9. Kimvula, J.M., Luzolo, J.T.T., Muke, M.K., Tango, E.K., & Ayingweu, C.L. (2023). Dynamique de l'occupation du sol à la station forestière de l'INÉRA Kiyaka, Kwilu, République Démocratique du Congo [Land-use dynamics at the INÉRA Kiyaka forest station, Kwilu, Democratic Republic of the Congo]. VertigO - la revue électronique en sciences de l'environnement. DOI : https://doi.org/10.4000/vertigo.40368.
10. Kobenan, K.R., & N'Guéssan, K.F. (2021). Analyse de l'occupation du sol et de l'impact des activités anthropiques sur le milieu naturel à Nassian (Côte d'Ivoire) [Analysis of land use and the impact of human activities on the natural environment in Nassian (Côte d'Ivoire)]. International Journal of Innovation and Scientific Research, 52(2), pp. 255-264.
11. Koné, M., Kouadio, Y. L., Neuba, D. F. R., Malan, D. F., & Coulibaly, L. (2014). Évolution de la couverture forestière de la Côte d'Ivoire des années 1960 au début du 21e siècle [Changes in forest cover in Côte d'Ivoire from the 1960s to the beginning of the 21st century]. International Journal of Innovation and Applied Studies, 7(2), 782-794.
12. Konan, K.E., Kangah, A., & Atta, J.M. (2016). Facteurs anthropiques et dynamique d'occupation des terres dans le parc national de la Comoé, en Côte d'Ivoire [Human factors and land-use dynamics in

Comoé National Park, Côte d'Ivoire]. Revue de Géographie de l'Université Ouaga I Pr Joseph KI-ZERBO, 5(2), 152-166.
13. Kouassi, K.D. (2008). Forêts classées de Côte d'Ivoire : la conservation à l'épreuve des modes d'appropriation [Classified forests of Côte d'Ivoire : Conservation challenged by patterns of appropriation]. Doctoral dissertation, Université de Bordeaux 2 et Université de Bouaké.
14. Kouassi, V.K.M., Kam, O., & Kra, T.O.K. (2023). Politique de gestion et dégradation persistante des aires naturelles protégées en Côte d'Ivoire : cas de la forêt classée de l'Anguédédou [Management policy and persistent degradation of protected natural areas in Côte d'Ivoire : The case of the Anguédédou Classified Forest]. VertigO, 23(1), 1–24. https://doi.org/10.4000/vertigo.39616.
15. Malan, D.F., Kougbo, M.D., Dogba, M., & Konan, A.S. (2023). Dynamique Spatio-Temporelle et Intérêt Pour la Conservation de la Forêt Classée de Goin-Débé, Une Aire Protégée Menacée de Disparition à l'Ouest de la Côte d'Ivoire [Spatiotemporal dynamics and conservation value of the Goin-Débé Classified Forest, a protected area threatened with disappearance in western Côte d'Ivoire]. European Scientific Journal, ESJ, 19(30). https://doi.org/10.19044/esj.2023.v19n30p231.
16. Menon, S., & Bawa, K.S. (1997). Application of geographic information systems, remote sensing, and landscape ecology approach to biodiversity conservation in Western Ghats. Current Science, 73(2), 134–145. http://www.jstor.org/stable/24098267.
17. Narendra Prasad, S. (1998). Conservation planning for the Western Ghats of Kerala : II. Assessment of habitat loss and degradation. Current Science, 75(3), 228-235. http://www.jstor.org/stable/24100956.
18. N'Dri Ehikpa, M.M., Kouassi, R.H., N'Guéssan, A.E., & Kassi N'Dja, J. (2020). Biodiversité végétale et dynamique et reconstitution des jachères post-culturales dans la forêt classée d'Irobo (Sikensi, Côte d'Ivoire) [Plant biodiversity, dynamics, and regeneration of post-cultivation fallows in the Irobo Classified Forest (Sikensi, Côte d'Ivoire)]. Agronomie Africaine, 32(2), 183–198.
19. Nourtier, M., & Grinand, C. (2016a). Analyse de la déforestation et ses agents, causes et facteurs sous-jacents. Rapport final MIKEA de composante 1 : Analyse historique de la déforestation dans la zone d'étude entre 1990 – 2015 [Analysis of deforestation and its agents, causes, and underlying factors. MIKEA Component 1 final report: Historical analysis of deforestation in the study area between 1990 and 2015].Banque mondiale & WCS.

https://www.nitidae.org/actions/parc-mikea-etude-sur-la-deforestation-historique-et-scenarios-de-deforestation-future

20. Nourtier, M., & Grinand, C. (2016b). Analyse de la déforestation et ses agents, causes et facteurs sous-jacents. Rapport final MIKEA de composante 2 : Analyse des agents, causes et facteurs de la déforestation et réalisation de projections des futurs taux de déforestation sous différents scénarios [Analysis of deforestation and its agents, causes, and underlying factors. MIKEA Component 2 final report : Analysis of the agents, causes, and factors of deforestation and projections of future deforestation rates under different scenarios]. Banque mondiale & WCS. https://www.nitidae.org/actions/parc-mikea-etude-sur-la-deforestation-historique-et-scenarios-de-deforestation-future
21. O'Neill, R.V., Hunsaker, C.T., Timmins, S.P., Jackson, B.L., Jones, K.B., Riitters, K.H., & Wickham, J.D. (1996). Scale problems in reporting landscape patterns at the regional. Landscape Ecology, 11, 169-180. https://doi.org/10.1007/BF02447515.
22. Perraud, A. (1971). Les sols [Soils]. In Le milieu naturel de la Côte d'Ivoire. (Mémoires de l'ORSTOM No. 50, pp. 269-389). ORSTOM.
23. Puyravaud, J.-P. (2003). Standardizing the calculation of the annual rate of deforestation. Forest Ecology and Management, 177, 593-596. https://doi.org/10.1016/S0378-1127(02)00335-3
24. Tao, S., Chave, J., Frison, P. L., Le Toan, T., Ciais, P., Fang, J., Wigneron, J.-P., Santoro, M., Yang, H., Li, Y., Labrière, N., & Saatchi, S. (2022). Increasing and widespread vulnerability of intact tropical forests to repeated droughts. Proceedings of the National Academy of Sciences of the United States of America, 119(37), e2116626119. https://doi.org/10.1073/pnas.2116626119.
25. Vancutsem, C., Achard, F., Pekel, J.-F., Vieilledent, G., Carboni, S., Simonetti, D., Gallego, J., Aragão, L. E. O. C., & Nasi, R. (2021). Long-term (1990-2019) monitoring of forest cover changes in the humid tropics. Science Advances, 7, eabe1603. https://doi.org/10.1126/sciadv.abe1603.
26. Vieilledent, G., Grinand, C., & Vaudry, R. (2013). Forecasting deforestation and carbon emissions in tropical developing countries facing demographic expansion : A case study in Madagascar. Ecology and Evolution, 3(6), 1702-1716. https://doi.org/10.1002/ece3.550.